WBP2 Negatively Regulates Hippo Pathway By Competitively Binding To WWC3 With LATS1 To Promote The Malignant Phenotype Of Non-Small Cell Lung Cancer

Qiang Han
College of Basic Medical Sciences and the First Affiliated Hospital of China Medical University
Xuezhu Rong
The First Affiliated Hospital of China Medical University
Xu-Yong Lin (linxuyong@hotmail.com)
China Medical University https://orcid.org/0000-0001-6714-0639
Xiupeng Zhang
China Medical University
Chuifeng Fan
China Medical University
Huanyu Zhao
China Medical University
Enhua Wang
China Medical University

Research

Keywords: WBP2, WWC3, LATS1, Hippo pathway, NSCLC, Invasion and metastasis

Posted Date: December 2nd, 2020

DOI: https://doi.org/10.21203/rs.3.rs-117703/v1

Abstract

Background: WW domain binding protein-2 (WBP2) can function as a YAP/TAZ co-activator and play a vital role in promoting breast cancer progression. However, the expression and potential molecular mechanism of WBP2 in the context of lung cancer are not fully understood.

Methods: Expression and subcellular localization of WBP2 in clinical samples and in lung cancer cell lines were analyzed with respect to various clinical pathological parameters using Chi-square tests. We used a series of cell function experiments and tumor formation experiments in nude mice to verify the effect of WBP2 on tumor cell proliferation and invasion. Dual-directional regulation of WBP2 expression, immunoprecipitation, luciferase reporter assays, and quantitative PCR analyses were used to explore the regulatory mechanisms and identify associated molecular markers.

Results: We determined that WBP2 was highly expressed in lung cancer specimens and cell lines and that this expression was closely related to the pTNM stage, lymph node metastasis, and poor prognosis of patients. Additionally, gain and loss of function experiments revealed that WBP2 could significantly promote the proliferation and invasion of lung cancer cells both *in vivo* and *in vitro*. To elucidate the underlying molecular mechanism, we determined that wild-type WBP2 could competitively bind to the WW domain of WWC3 with LATS1 through its PPxY motifs to inhibit the formation of the WWC3-LATS1 complex, reduce the phosphorylation level of LATS1, and ultimately promote YAP nuclear translocation to suppress the activity of the Hippo pathway.

Conclusions: From the aspect of upstream molecules of Hippo signaling, WBP2 promotes the malignant phenotype of lung cancer cells in a unique manner that is not directly dependent upon YAP, thus providing a corresponding experimental basis for the development of targeted therapeutic drugs for lung cancer.

Background

The Hippo pathway was initially identified in Drosophila, and this pathway is highly conserved in the evolution of species, where it plays a crucial role in maintaining homeostasis and regulating cell proliferation, differentiation, apoptosis, and other physiological processes. Increasing numbers of studies have confirmed that disorders in Hippo activity lead to tumor formation and progression [1, 2]. In the classical Hippo pathway, the molecular composition usually includes upstream molecules, such as Fat-cadherin, Merlin, WWCs, and AMOT protein, a central kinase complex (MST1/2-SAV-LATS1/2-MOB), and downstream effective molecules (YAP protein and its homolog TAZ). The target genes of the Hippo pathway typically include *CTGF*, *CYR61*, and other related genes. When the Hippo pathway is activated, the upstream molecules induce cascade phosphorylation of the central kinase MST-LATS complex. Increases in LATS phosphorylation levels can promote the phosphorylation of YAP, and this protein remains in the cytoplasm, binds to the 14-3-3 protein, and is then degraded by the ubiquitin proteasome pathway. However, when the Hippo pathway is inhibited, YAP escapes from the protease and

accumulates within the cytoplasm, after which, YAP translocates into the nucleus to bind to the transcription factor TEADs to activate the transcription of Hippo target genes [3–5].

WW domain binding protein-2 (WBP2) was initially identified as a homologous ligand protein of the YAP-WW domain and was demonstrated to interact with the pair box gene (PAX8) transcription factor with unknown function [6–9]. Currently, a number of studies have focused on the molecular function of WBP2 in human solid tumors by assessing the impact of this protein on the biological phenotype of breast cancer. For example, in breast cancer, WBP2 is highly expressed and is significantly associated with poor prognosis [10, 11]. WBP2 can bind to estrogen and progesterone receptors and can act as a co-activator of estrogen receptor (ER) and progesterone receptor (PR) hormone signaling transduction [12–15]. Additionally, the synergetic effect of WBP2 and YAP/TAZ in the nucleus plays an important role in promoting the proliferation and invasion of breast cancer cells by regulating the activities of classical signal pathways in both tumor tissues and normal tissues [16–20]. However, the expression pattern of WBP2 in lung cancer and the ability of this protein to regulate the activity of the Hippo pathway in an indirect manner that is dependent upon YAP both remain unreported.

WW and C2 domain-containing protein-3 (WWC3) belongs to the WWC family (KIBRA/WWC1, WWC2, and WWC3) that serves as the classic upstream protein molecules in the Hippo pathway. Joachim et al. observed that WWCs could activate Hippo pathway activity by binding to the PPxY motif of LATS kinase via the WW domain to promote LATS1 auto-phosphorylation [21, 22]. Our previous studies further demonstrated that WWC3 also regulates the activities of both the Hippo and Wnt pathways primarily through interactions with LATS and DVLs that is facilitated by the WW domain and that WWC3 plays an important role in inhibiting the malignant phenotype of lung cancer [23, 24]. Based on literature reviews and the results of our previous studies, we speculate that the PPxY motif within the structure of WBP2 may also bind to the WW domain of WWC3 to regulate the activity of Hippo pathways at the upstream level through a non-direct YAP/TAZ-dependent pathway.

In this study, we detected the expression and subcellular localization of WBP2 in clinical samples and in lung cancer cell lines and then analyzed the relationship of this expression to various clinical pathological parameters. Second, we verified the effect of WBP2 on tumor cell proliferation and invasion using a series of cell function experiments and tumor formation experiments in nude mice. Dual-directional regulation of WBP2 expression, immunoprecipitation, luciferase reporter assays, and quantitative PCR analyses were applied to explore the specific regulatory mechanism of WBP2 in the context of the Hippo pathway, and this provided an experimental basis for the identification of molecular markers of lung cancer and the development of targeted therapeutic drugs.

Material And Methods

Patient information and specimens

This study was approved by the ethics committee of China Medical University and was performed according to the requirements of the Declaration of Helsinki. All lung cancer patients who participated in this study were aware of the study and signed an informed consent form. A total of 127 lung cancer specimens and 32 normal lung tissue samples were collected from the Department of Pathology of the First Affiliated Clinical Hospital of China Medical University. None of the patients received chemotherapy or radiotherapy prior to the operation. There were 79 men and 48 women included in this study, and the average age of the participants was 60 years (range, 45–83 years). According to the 2015 lung cancer classification standard [25], 99 cases were classified as stage I–II and 28 cases were classified as stage III. Among the 127 lung cancer patients examined, complete follow-up data were obtained for 93 patients.

Immunohistochemistry

All tissues were fixed using neutral formaldehyde, embedded in paraffin, and then sectioned to 4 μm thickness. S-P immunohistochemical staining was used. Slides were incubated with polyclonal rabbit-derived WBP2 antibody (HPA065682, 1:50, Sigma-Aldrich, St. Louis, MO, USA) at 4 °C overnight. Phosphate buffered-saline (PBS) was used as a negative control. After incubation at 37 °C for 30 min, the sections were DAB stained. Five visual fields were randomly selected from each tissue section, and 100 tumor cells were counted in each field. According to the percentage of cells stained, the expression of WBP2 was divided into five grades that included 0 (no staining), 1 (1–25%), 2 (26–50%), 3 (51–75%), and 4 (more than 75%). According to the intensity of cell staining, the expression of WBP2 was divided into three grades that included 0 (no staining), 1 (light yellow particles), and 2 (dark yellow or yellow brown particles). Each tissue section corresponds to a percentage fraction and a color fraction. When these two parameters are multiplied, the product is the final score of the slice. We evaluated the expression of WBP2 in normal lung tissue located adjacent to the tumor using this scoring standard. We observed that the expression intensity of WBP2 in most cases was greater than 4. Therefore, we defined expression of WBP2 that was less than 4 as negative expression (-), while 4–5 was considered weakly positive (+), 6–7 was moderately positive (++), and ≥ 7 was strongly positive (+++).

Western blot

Cells were fully lysed using RIPA buffer (Beyotime Biotechnology, Shanghai, China), and the total protein was then extracted. The protein was quantified using the BCA method (Beyotime Biotechnology, Shanghai, China). The total protein (40 μg) was electrophoresed by SDS-PAGE at 8% and 10% concentrations, and the proteins were then transferred to PVDF membranes (GE Healthcare, Waukesha, WI, USA). The membranes were then incubated in skimmed milk powder (5%) (BD Biosciences, Lexington, KY, USA) for 1 h. The membranes were then incubated with the indicated primary antibodies at 4 °C overnight. The primary antibodies used for these experiments included WBP2 (#11831, IB/1:1000), Myc-Tag (#2276, IB/1:1000, IP/1:50), FLAG-Tag (#14793, IB/1:1000, IP/1:50), MST (#3682, IB/1:1000), p-MST (#49332, IB/1:1000), p-LATS1 (#8654, IB/1:1000), LATS1 (#3477, IB/1:1000), p-YAP (#13008, IB/1:1000), YAP (#14074, IB/1:1000), and actin (#3700, IB/11000) and were purchased from Cell Signaling Technology. Inc. (Danvers, MA, USA). WWC3 (HPA039814, IB/1:500) was purchased from Sigma-Aldrich; GAPDH (sc-293335, IB/1:1000) was purchased from Santa Cruz Biotechnology Inc. (CA, USA); and GFP-

Tag (#JL-8, IB/1:3000) was purchased from Clontech (TaKaRa-Bio, Beijing, China). After primary antibody staining, membranes were incubated with goat anti-rabbit secondary antibody (IB/1:5000, Cell Signaling Technology) at 37 °C for 1 h. Immunoreactive bands were detected with ECL luminescence; the expression of GAPDH was used as the relative loading control. All experiments were repeated in triplicate.

Cell lines

The immortalized human bronchial epithelial cell line (HBE) was purchased from the American Type Culture Collection (ATCC, Manassas, VA, USA). The human non-small cell lung cancer cell (NSCLC) lines H661, H1299, A549, and Calu-1 were purchased from Shanghai Cell Bank of the Chinese Academy of Sciences (Shanghai, China). The LK2 cell line was kindly provided by Prof. Hiroshi Kijima (Department of Pathology and Bioscience, Hirosaki University Graduate School of Medicine, Japan). All cells were cultured in either Dulbecco's modified Eagle medium (DMEM, Hyclone, Logan, UT, USA) or Roswell Park Memorial Institute-1640 (RPMI-1640, Hyclone) medium supplemented with 10% fetal bovine serum (FBS, Hyclone) at 37 °C in a humidified atmosphere at 5% CO_2. All cell lines were authenticated by short tandem repeat DNA profiling.

Plasmid construction and transfection

Myc/DDK-tagged-pCMV6 empty vector and Myc/DDK-tagged-pCMV6-WBP2 plasmids were purchased from Origene (product No. PS-100001 and RC-203955, respectively, Rockville, MD, USA). PcDNA3.1 empty vector and pcDNA3.1-FLAG-LATS1 were constructed by BaiHao Biotechnology Company (Shenyang, China). pEGFP-C2 empty vector and p-EGFP-C2-WWC3 were provided by Professor Joachim Kremerskothen of Muenster University, Germany. ShRNA-control, shRNA-WBP2-1#, shRNA-WBP2-2#, and shRNA-WBP2 were coated with lentivirus by the Genechem Company (Shanghai, China). Control siRNA (sc-37007), siRNA-WBP2 (sc-93955), and siRNA-LATS1 (sc-35546) were purchased from Santa Cruz Biotechnology. p2xFlag-YAP1 (#17791) and pGL3b_8xGTIIC-luciferase (#34615) were purchased from Addgene (Cambridge, MA, USA). The pRL-TK vector (#E2241) was purchased from Promega (Madison, WI, USA). Lipofectamine 3000 (Invitrogen, Carlsbad, CA USA) was used for transient transfection. Stable transfection was screened for using purinomycin and G418 (Sigma-Aldrich).

Immunofluorescence assay

The cells were fixed using 4% paraformaldehyde and incubated with 3% BSA for 1 h at 25 °C. WBP2 antibody (#HPA065682, 1:25, Sigma-Aldrich), WWC3 antibody (#HPA039814, 1:50, Sigma-Aldrich), and YAP antibody (#14074, 1:50, Cell Signaling Technology) were used for overnight incubation at 4 °C, and the cells were then incubated with fluoresceine isothiocyanate (FITC) or tetramethyl rhodamine isothiocyanate (TRITC)-labeled goat anti-rabbit/mouse antibody (ZSGB-Biotechnology company, Beijing, China) for 1 h at 25 °C. The nuclei were stained using 2-(4-Amidinophenyl)-6-indolecarbamidine dihydrochloride (DAPI) staining solution and scanned using a radiance 2000 laser confocal microscope (Carl Zeiss, Thornwood, NY, USA).

MTT Assay

Approximately 3000 transfected cells were cultured in 10% serum in a 96-well plate, and 20 μL of 5 mg/mL MTT (thiazolyl blue) solution was added to each well. After incubation at 37 °C for 4 h, the solution was removed and the resulting MTT crystals were dissolved in 150 μL of DMSO. The absorbance peak at 490 nm was detected using a spectrophotometer.

Cell migration and matrix invasion assays

For the matrix invasion assay, the matrix adhesive (BD Biosciences) was diluted in the 24-well plate at a 1:3 ratio in DMEM medium that was free of fetal serum and antibiotics. The lung cancer cells were inoculated in the upper chamber at a density of 5×10^5 cells in 100 μL of medium without fetal serum, and culture medium containing 10% fetal serum (Hyclone) was placed in the lower chamber. After 24 h of cultivation, cells were fixed for 15 min using methanol, and hematoxylin staining was subsequently performed. Ten fields were randomly selected to count the number of invading cells. The experiment was repeated in triplicate, and the average value was acquired accordingly.

Colony formation experiment

The cells were transfected for 48 h and then inoculated into a 6-cm cell culture dish (1000 cells/plate) and incubated for 12 days. The cells were then washed with PBS (three times for five minutes) and subsequently stained using hematoxylin for 10 minutes before counts were performed; the experiments were repeated in triplicate to acquire an average value.

Co-immunoprecipitation

The cells were washed twice with 5 mL of PBS and then placed into an ice bath where they were lysed for 2 min using NP-40 buffer (Beyotime Biotechnology, Shanghai, China). Lysates were transferred from the culture plate to a new 1.5 ml Eppendorf tube. The supernatant was centrifuged for 15 min at 16,000 *g* and 4 °C. Protein concentrations were quantified using the BCA method (Beyotime Biotechnology), and the immune complex was collected for western blot analysis.

RNA extraction and quantitative PCR

The RNeasy Plus Mini Kit (Qiagen, Hilden, Germany) was used to extract total RNA from the cells. Quantitative PCR was performed using an ABI-7900 system (Applied Biosystems, Foster City, CA) with 20 μL SYBR Green PCR Master Mix (Takara, Tokyo, Japan). The PCR parameters were 95 °C for 30 s, 40 cycles at 95 °C for 5 s, and 60 °C for 30 s. *GAPDH* mRNA is used to normalize the relative expression of the target mRNAs. A dissociation step was applied to generate a melting curve to confirm primer specificity. The relative levels of gene expression were represented as $\Delta CT = CT_{gene}\text{-}CT_{reference}$, and the fold change in gene expression was calculated using the $2^{-\Delta\Delta CT}$ method. The experiments were repeated in triplicates. The primer sequences used for this study are listed in Table 1.

Table 1
Primers for real-time RT-qPCR

Primer sequences (5'→3')	
WBP2	5'-CAAGAGCGCATGTTGAAGGAA-3'
	5'-CGCTGCTGCTTAATCTGGTAGA-3'
CTGF	5'- AACTGCAACCTCTCGCACTG-3'
	5'- GCTCGGGCTCCTTGTAATTCT-3'
CYR61	5'- CTCGCCTTAGTCGTCACCC-3'
	5'- CGCCGAAGTTGCATTCCAG-3'
GAPDH	5'- GGAGCGAGATCCCTCCAAAAT-3'
	5'- GGCTGTTGTCATACTTCTCATGG-3'

GST-pulldown

The WWC3 protein coupled to a GST label was induced in *E. coli* BL21 (30 °C, 3 h, 200 rpm/min) and purified according to standard steps. The purified protein was recombined with glutathione sepharose (GE Healthcare, Waukesha, WI, USA) magnetic beads and then incubated with H1299 cell lysate transfected with Myc-WBP2 plasmid at 4 °C overnight. Finally, the complexes were detected by western blot and Coomassie brilliant blue staining.

Dual-luciferase reporter genes assay

Cells were co-transfected with either WBP2 plasmid or siRNA-WBP2 and with the YAP-associated transcription factor TEAD reporter pGL3b_8xGTIIC-luciferase (#34615, Addgene) in 24-well plates. Renilla luciferase was used as a signal normalization control. The assays were performed according to the manufacturer's protocol (Promega). Six independent transfections were performed for each experiment. The data were normalized to those for the empty vector control and are presented as average ± S.D.

Animal experiments

For the subcutaneous tumor formation experiment in nude mice, a total of 12 BALB/c nude mice (4 weeks old, female, 16–20 g, Specific Pathogen Free, SPF-standard) were purchased from Beijing Charles River company (Beijing, China). The food and drinking water were sterilized using a semi-barrier system at constant temperature and humidity. All animal experiments were performed in accordance with the ethical regulations of animal experiments at China Medical University. The tumor formation experiment was divided into four groups (three rats per group) that included H1299 cells stably transfected with empty plasmid, H1299 cells stably expressing WBP2, A549 cells stably transfected with shRNA-WBP2, and cells stably transfected with control shRNA. The cell concentration for each group was adjusted to 5×10^6 cells/mL, and 0.2 mL of cells was injected subcutaneously into the backs of nude mice. After 4

weeks of observation beginning from the day of injection, the mice were euthanized, and the weights and volumes of the subcutaneous tumors were recorded accordingly.

For the intrapulmonary metastasis experiment, the mice were divided into four groups (eight rats per group) that were the same as the groups used for the subcutaneous tumor formation experiment. The numbers and sizes of the metastatic foci in the lungs were recorded. After six weeks, the lungs were removed and fixed using 10% neutral formalin. Paraffin-embedded sections were prepared and stained with hematoxylin and eosin (H&E).

Statistical analysis

All data were analyzed using SPSS22.0. Chi-square tests were used to test the correlation between WBP2 expression and clinicopathological factors. The student's *t*-test was used to analyze differences between groups. A $P < 0.05$ was considered as statistically significant.

Results

WBP2 is highly expressed in NSCLC and is associated with poor prognosis

To explore if WBP2 plays a specific role in NSCLC, we first detected the expression of WBP2 in samples of lung tissue from lung cancer patients and investigated the association of this expression with the survival and prognosis of patients with lung cancer via immunohistochemistry staining. Our results indicated that in terms of localization, WBP2 was localized in the cytoplasm of lung cancer cells, whereas with regard to expression, WBP2 was poorly or even negatively expressed in normal cells (71.9%, 23/32) (low expression in normal bronchial epithelial cells, negative expression in normal alveolar epithelium) but highly expressed in lung adenocarcinoma and squamous cell carcinoma (55.2%, 70/127, Fig. 1-A) Additionally, the expression difference between para-cancerous and cancerous tissues was significant ($P < 0.05$, Fig. 1-B). Notable, the expression of WBP2 in patients with lymph node metastasis was significantly higher than that observed in patients without lymph node metastasis (44.7% *vs.* 70.6%, $P < 0.05$, Fig. 1-A, B). The chi-square test revealed that high expression of WBP2 was closely related to advanced pTNM stage ($P = 0.001$) and positive lymph node metastasis ($P = 0.006$) in patients with NSCLC (Table 2). Cox univariate and multivariate analyses indicated that a high TNM stage, adenocarcinoma histological type, and high WBP2 expression ($P = 0.038$, $P = 0.017$ and $P = 0.030$, respectively; Table 3) were all independent prognostic factors in NSCLC. Accordingly, western blot analyses showed that the expression level of WBP2 in lung cancer tissues was also significantly higher than that in adjacent tissues (14/16, Fig. 1-C, D). The online network database (http://www.kmplot.com) suggested that high WBP2 expression negatively correlated with overall survival (OS) and progression-free survival (FP) ($P = 0.0066$, and $P = 0.015$, respectively; Fig. 1-E, F); our Kaplan–Meier survival analysis also verified these results ($P < 0.05$, Supplementary Figure S1). When the lung cancer cell lines were compared to the normal bronchial epithelial cell line HBE, we determined that WBP2 was also highly expressed in the four lung cancer cell lines (n = 5), and immunofluorescence staining revealed that WBP2 was located in the cytoplasm of lung cancer cells (Supplementary Figure S2). This finding was consistent

with the results obtained using clinical tissue specimens. Based on the above results, we can conclude that WBP2 may play a role in promoting malignancy by functioning as an oncogene.

Table 2
Association of WBP2 expression with clinical and pathological characteristics in NSCLC

Clinicopathological characteristics	N	Positive	Negative	χ2	P(two-side)
Age (years)					
<60	37	25	12	3.271	0.080
≥60	90	45	45		
Gender					
Male	79	43	36	0.040	0.856
Female	48	27	21		
Histological type					
Squamous cell carcinoma	54	32	22	0.651	0.473
Adenocarcinoma	73	38	35		
Differentiation					
Well	40	22	18	0.000	1.000
Moderate & Poor	87	48	39		
TNM classification					
□ + □	99	47	52	10.604	0.001*
□	28	23	5		
Lymph node metastasis					
Positive	51	36	15	8.245	0.006*
Negative	76	34	42		
*: $P < 0.05$, statistically significant					

Table 3
Summary of Cox univariate and multivariate regression analysis of the association between clinicopathological characteristics and overall survival in 93 cases of non-small cell lung cancer

Clinicopathological	**Hazard ratio**	***P***
characteristics	(95% CI)	
Univariate analysis		
Age older than 60	0.534 (0.286–1.032)	0.062
Gender: male	0.973 (0.515–1.839)	0.934
Histological type: Adenocarcinoma	0.450 (0.237–0.855)	0.015*
Poor differentiation	1.906 (0.968–3.754)	0.062
High TNM classification	3.768 (1.908–7.444)	0.000*
Positive lymph node metastasis	2.713 (1.445–5.096)	0.002*
Positive WBP2 expression	3.274 (1.599–6.701)	0.001*
Multivariate analysis		
Histological type : Adenocarcinoma	0.431 (0.216–0.860)	0.017*
High TNM classification	2.756 (1.058–7.179)	0.038*
Positive WBP2 expression	2.294 (1.082–4.867)	0.030*

Ectopic expression of WBP2 promotes the proliferation, migration, and invasion of NSCLC cells both in vitro and in vivo

As numerous studies have indicated that WBP2 plays an essential role in promoting tumor progression in breast cancer, we attempted to explore if WBP2 can exert an underlying impact on the malignant phenotype of tumor cells in NSCLC. As shown in Figure-1E, WBP2 expression was the highest in A549 cells lines but was relatively low in H1299 cells. Therefore, we selected the H1299 cell line for the overexpression experiments. The colony formation assay showed that in comparison with that of the control group, the proliferative abilities of H1299 cells were significantly enhanced after stable transfection of WBP2 (Fig. 2-A). Additionally, we found that WBP2 overexpression promoted the migration and invasiveness of lung cancer cells (Fig. 2-B, C). These experimental results indicated that WBP2 possessed the ability to promote the malignant phenotype of tumors *in vitro*. To further verify if WBP2 exerts similar effects *in vivo*, we performed subcutaneous tumor transplantation experiments and lung metastasis experiments based on tail vein injections in nude mice, and found that in comparison with those of control group, the volumes and weights of the subcutaneous tumors (Fig. 2-D,E) and the number of metastatic foci (Fig. 2-F,G) in the lungs of mice stably overexpressing WBP2 were significantly increased, which was consistent with the results obtained *in vitro*.

WBP2 knockdown weakens the malignant phenotype of lung cancer cells both in vivo and in vitro

We further attempted to detect any changes in the biological functions of the lung cancer cells after WBP2 knockdown. For these experiments, we used lentivirus-coated shRNA-WBP2 to transfect the A549 cell line with high WBP2 expression. Using colony formation, cell migration, and matrix invasion assays, we found that in contrast to the results of the functional experiments, weakened proliferative, migratory, and invasive abilities were observed in A549 cells after WBP2 knockdown (Fig. 3-A, B, C). *In vivo*, we found that the volumes and weights of subcutaneous transplanted tumors derived from A549 cells transfected with lentivirus-shRNA-WBP2 in nude mice were significantly lower than those derived from control mice (Fig. 3-D,E) and that the number of lung metastases induced by caudal vein metastasis was also significantly reduced (Fig. 3-F,G). Therefore, combined with the results of the *in vivo* and *in vitro* experiments, we can conclude that WBP2 functions as a tumor promoting factor when exerting its potential biological functions in lung cancer cells.

WBP2 is a negative regulator of the Hippo signaling pathway in lung cancer cells

It is currently unclear exactly how WBP2 affects the biological function of lung cancer cells. In breast cancer, WBP2 has been reported to inhibit the occurrence and development of breast cancer by inhibiting the activity of the Hippo pathway. Based on this, we first examined the effect of WBP2 on Hippo pathway activity in the context of lung cancer cells. Initially, a dual-luciferase reporter assay was used to demonstrate that WBP2 overexpression in H1299 could significantly upregulate YAP-induced transcriptional activity of the TEAD reporter assay. Specifically, the activity of the Hippo pathway was inhibited (Fig. 4A-a). In contrast, the transcriptional activity of the TEAD reporter gene was downregulated by siRNA-WBP2 transfection in A549, indicating that the Hippo pathway was activated (Fig. 4A-b). Cascade phosphorylation of the MST-LATS complex in the Hippo pathway plays a central role in classical Hippo activation. However, the impact of WBP2 on MST and LATS phosphorylation has not been previously elucidated. To address this, we performed western blot analyses to explore the effect of WBP2 on the phosphorylation of these two kinases. The results indicated that the phosphorylation levels of LATS1 and YAP were significantly downregulated in response to WBP2 overexpression; however, the phosphorylation levels and total amounts of MST did not exhibit any significant changes (Fig. 4B), suggesting that WBP2 affected the phosphorylation of LATS1 and regulated the activity of the Hippo pathway in an MST-independent manner. We further assessed the changes in the transcription levels of *CTGF* and *CYR61* in Hippo pathway target genes using RT-qPCR. We found that the transcription levels of *CTGF* and *CYR61* were significantly upregulated after transfection with WBP2 (Fig. 4C-a), and the results were the opposite in response to silencing of WBP2 (Fig. 4C-b). The GEPIA online correlation database (gepia.cancer-pku.cn) also revealed a positive association between WBP2 and YAP target genes, including *CTGF*, *CYR61*, and *AREG* (Supplementary Figure S3). The import of YAP into the nucleus is a direct indicator of Hippo pathway inactivation, and laser confocal detection assays revealed that the level of YAP within the nucleus was increased after transfection with WBP2 (Fig. 4D). These results indicate that WBP2 promotes YAP translocation into the nucleus by inhibiting LATS1 phosphorylation, and this ultimately inhibits Hippo pathway activity.

The upstream protein WWC3 of the Hippo pathway was identified as WBP2 binding protein

Previous studies suggested that WBP2 localizes within the nucleus of breast cancer cells and acts as a co-activator of YAP to promote the transcription of downstream genes [17]. Interestingly, we found that WBP2 was localized within the cytoplasm of lung cancer cells, and based on this, we speculated that WBP2 may modulate the Hippo pathway in a YAP-indirect-dependent manner. This knowledge combined with our previous results indicated that WBP2 can downregulate LATS1 phosphorylation levels, and we therefore focused our studies on the upstream protein molecules that can cause changes in LATS1 phosphorylation levels. The WWCs protein family contains the classical upstream molecules of the Hippo pathway that can interact with LATS1 and promote LATS1 phosphorylation. Our previous studies also confirmed the important role of WWC3 in lung cancer [22, 23]. In this study, immune-co-precipitation and GST-pulldown assays were performed to verify that WBP2 can dramatically interact with the upstream protein WWC3, and our results indicate that these proteins can directly interact (Figure. 5A, B). Confocal laser scanning revealed the co-localization of WBP2 and WWC3 in the cytoplasm of A549 cells that possess high expression levels of both proteins (Fig. 5C). To further explore the structural basis underlying the binding of WBP2 and WWC3 [23], we constructed a series of WBP2 (deletion of PPxY motifs) and WWC3 mutants (deletion of double WW domains) and then transfected them into H1299 cells, as these cells exhibited high transfection efficiency. Additionally, immunoprecipitation studies indicated that WBP2 was bound to the WW domain of WWC3 through its PPxY motifs (Fig. 5D).

WBP2 inhibits the activity of the Hippo pathway by inhibiting the phosphorylation of LATS1 via interaction with WWC3

WWC3 can activate the Hippo pathway by binding of the WW domain in competition with LATS1 kinase to promote LATS1 phosphorylation; WBP2 can also combine with the WW domain of WWC3 via PPxY motifs. Therefore, the binding of the PPxY motifs of WBP2 to the WW domain of WWC3 led us to speculate that WBP2 may competitively bind to the WW domain of WWC3 with LATS1 to weaken the activity of the WWC3-LATS1 complex. To verify this possibility, we first increased the expression of WBP2 in H1299 cells that exhibit low WWC3 and WBP2 expression and high LATS1 expression [26]. In these cells, immunoprecipitation experiments showed that the binding of WWC3 and LATS1 gradually decreased in response to WBP2 overexpression in a dose-dependent manner (Fig. 6A). Conversely, the binding ability of LATS1 to WWC3 was dramatically increased after WBP2 knockdown in A549 cells (low expression of LATS1 and high expression of WWC3 and WBP2) (Fig. 6B). Conversely, we overexpressed LATS1 in A549 cells and found that the binding of WBP2 and WWC3 gradually decreased (Fig. 6C); however, after LATS1 was knocked down in H1299, the binding of WBP2-WWC3 gradually increased in a dose-dependent manner (Fig. 6D). These results clearly demonstrate that WBP2 competitively binds to WWC3 with LATS1. Next, we explored the underlying impact of this competitive interaction between these three factors on the Hippo pathway. First, by using a dual-luciferase reporter assay, we found that the ectopic expression of WBP2 in H1299 cells significantly rescued the decrease in YAP-TEAD transcriptional activity caused by WWC3 (Fig. 6E). However, after knockdown of WBP2 in A549 cells, the inhibition of Hippo induced by LATS1 was further promoted (Fig. 6F). In contrast, overexpression of

LATS1 could dramatically reduce the increase in YAP-TEAD activity that was induced by WBP2 (Fig. 6G), and this effect was reversed after LATS1 knockdown (Fig. 6H). Accordingly, western blot analyses also revealed that WBP2 overexpression significantly reversed the upregulation of LATS1 and YAP phosphorylation that was induced by WWC3 in H1299 cells, and this effect was abrogated after WBP2 knockdown (Fig. 6I, J). Based on the above results, we believe that WBP2 is competitive with LATS1 for binding to WWC3, and this competitive binding results in a decrease in WWC3-LATS binding and eventually leads to downregulation of LATS1 phosphorylation to inhibit the activity of the Hippo pathway.

Discussion

Currently, increasing numbers of studies have reported the carcinogenic effect of WBP2 in human solid tumors, particularly from breast cancer. For example, WBP2 can promote G1/S phase transformation of breast cancer cells and can accelerate cell cycle progression [27]. WBP2 can also promote the proliferation and invasion of triple negative and non-triple negative breast cancer cells through ER/PR-dependent or independent mechanisms, and adverse prognosis for breast cancer patients and their treatment sensitivity to chemotherapy drugs have also been closely correlated to WBP2 status [11–15, 28, 29]. Additionally, WBP2 can interact with α-enolase (ENO-1) and Homer protein homolog-3 (homer-3) in glioma and can promote the malignant phenotype of glioma cells through the ENO-1-PI3K-AKT signaling pathway and the glycolysis pathway [30]. However, the expression of WBP2 in NSCLC and the potential molecular mechanisms of action for WBP2 have not been reported.

In this study, we found that WBP2 was highly expressed in NSCLC and was associated with poor prognosis of patients. Moreover, WBP2 promoted the proliferation, migration, and metastasis of lung cancer cells *in vivo* and *in vitro*. This was consistent with the basic function of WBP2 in breast cancer and other malignant solid tumors. However, the cause of high expression of WBP2 in lung cancer remains unclear. According to the existing literature, the expression of WBP2 could be affected by many underlying factors. In hepatocellular carcinoma, micro non-coding RNA (miRNA) can affect the malignant phenotype of hepatocellular carcinoma cells by downregulating the expression of WBP2 [31]. The transcription factor USF1 can promote the transcription of WBP2 by binding to the E-box region of the WBP2 promoter [32]. ITCH also attenuated CD4 T-cell proliferation in mice by limiting WBP2 protein stability [33]. Additionally, changes in the activity of some classic signaling pathways can play an important role in regulating the expression of WBP2. For example, MST in the Hippo pathway can regulate the expression of WBP2 through the miRNA-Dicer pathway in a kinase-dependent manner [34]. Wnt pathway activation inhibits the degradation of WBP2 mediated by Itch in a post-translational manner, thus affecting the biological phenotype of breast cancer [18]. These experimental data have aided in clarifying the reasons for the high expression of WBP2 in different tumors. In regard to the high expression of WBP2 in lung cancer, it remains unclear if this is related to the amplification of gene promoter, transcription level, or post-translation regulation. Based on this, these factors should be explored in follow-up research studies.

The molecular mechanism underlying the function of WBP2 in breast cancer is closely related to the steroid hormone signaling pathway (ER-based). Some scholars have determined that WBP2 is also the key node of the PI3K and Wnt signaling transduction pathways in other tumors [14, 18, 29], and WBP2 also plays a key role in the Hippo pathway [34]. Both Yki/YAP and TAZ in the Hippo signaling pathway are vital binding proteins of WBP2, as the binding of these proteins facilitates the transcription of downstream target genes and affects the development of Drosophila and the proliferation and invasion of tumor cells [8–9, 16, 19–20]. In NSCLC, inactivation of the Hippo pathway is also a common phenomenon that is closely related to the occurrence, development, and drug resistance of lung cancer [35]. Therefore, we also focused on exploring if the potential molecular mechanism of WBP2 in lung cancer is related to Hippo signaling.

First, we used luciferase reporter gene assays and RT-qPCR to verify that WBP2 could promote YAP translocation into the nucleus to upregulate YAP/TEAD transcriptional activity and promote the transcription of the target genes *CTGF* and *CYR61*. This dual-directional regulation of WBP2 expression confirmed the negative regulatory effect of WBP2 on the Hippo pathway in lung cancer cells. However, interestingly, we found that WBP2 was localized within the cytoplasm of lung cancer cells according to immunohistochemical staining and cell fluorescence, which is in contrast to previous reports that suggested that WBP2 was a co-activator of YAP/TEAD in the nucleus. Thus, WBP2 may modulate Hippo in an indirect YAP/TAZ-dependent manner in the cytoplasm by facilitating upstream molecular processes. When investigating this hypothesis, we used immunoprecipitation and GST-pulldown assays to show that WBP2 could directly bind via the PPxY motifs to the WW domain of WWC3 upstream of the Hippo pathway. WWC3 promotes the autophosphorylation of LATS1 via the MST-independent pathway, activates the Hippo pathway, and inhibits the proliferation and migration of lung cancer cells [24] and promotes Earle's balanced salt solution (EBSS)-induced apoptosis and inhibits cell growth by inhibiting the autophagy process [36]. Furthermore, WWC3 acts as a tumor suppressor in other tumors such as gastric cancer and glioma [37, 38]. We found that WBP2 competitively binds to the WW domain of WWC3 with LATS1 to inhibit the formation of the WWC3-LATS1 complex and reduces the phosphorylation level of LATS1 to promote YAP translocation into the nucleus. This inhibits the Hippo pathway and ultimately promotes the malignant phenotype of lung cancer. Therefore, WBP2 regulates Hippo activity in a manner that is not directly dependent on YAP at the upstream level, and this explains the specific molecular mechanism of the regulation of the Hippo pathway by WBP2 that is localized to the cytoplasm. In regard to the differences in subcellular localization of WBP2 in breast cancer and lung cancer, future research will determine if these differences are tissue-specific or regulated by other factors.

Conclusions

WBP2 is highly expressed in NSCLC and is closely related to tumor stage, lymph node metastasis, and poor prognosis in patients. The gain and loss function of experiments have clearly demonstrated that WBP2 can promote the proliferation and invasion of lung cancer cells and can function as an oncoprotein in lung cancer. Mechanistically, WBP2 promotes carcinogenesis through inhibiting the Hippo signaling pathway. WBP2 is a WW domain-binding protein that binds to the WW domain of WWC3

through via PPxY motifs, inhibits the formation of the WWC3-LATS1 complex, reduces LATS1 phosphorylation levels, promotes YAP accumulation and nuclear translocation, and finally inhibits Hippo signaling pathway activity to promote the malignant phenotype of lung cancer cells. These results not only reveal the role and mechanism of WBP2 in the formation and development of NSCLC, but they also provide an important experimental basis for developing new targeted drugs and explaining the mechanism of drug resistance.

Abbreviations

WBP2: WW domain binding protein-2; WWC3: WW and C2 domain containing protein-3; LATS: Large tumor suppressor; MST: Mammalian sterile-20-like; YAP: yes-associated protein; CTGF: connective tissue growth factor; CYR61: Cysteine-rich- 61; RT-qPCR: reverse transcription-quantitative polymerase chain reaction; GAPDH: glyceraldehyde-3-phosphate dehydrogenase; TEAD: TEA domain family protein; shRNA: short hairpin RNA; IgH: immunoglobulin heavy chain; IgL: immunoglobin light chain; GST: Glutathione-S-transferase; NSCLC: non-small cell lung cancer.

Declarations

Ethics approval and consent to participate

The study was approved by the Medical Research Ethics Committee of China Medical University, and informed consent was obtained from all patients. The nude mice used for this study were treated in accordance with the experimental animal ethics guidelines issued at China Medical University, and all experiments were approved by the Institutional Animal Research Committee of China Medical University.

Consent for publication

Not applicable.

Availability of data and materials

All data generated or analyzed during this study are included in this published article and supplementary information files. Further details are available from the corresponding author upon request.

Competing interests

The authors declare no conflict of interest.

Funding

This study was supported by the National Natural Science Foundation of China (No. 81902986 to Qiang Han; No.82003119 to Xuezhu Rong), the China Postdoctoral Science Foundation (2020M670816 to Xuezhu Rong), the Natural Science Foundation of Liaoning Province, China (20180530040 to Xuyong

Lin) and Natural Science Foundation of Xinjiang Autonomous Region (Province), China (2020D01A123 to Xuyong Lin).

Author contributions

Qiang Han and Xuezhu Rong designed the research studies, conducted experiments, acquired and analyzed data, and wrote the manuscript. Xiupeng Zhang, Chuifeng Fan and Huanyu Zhao conducted experiments, acquired and analyzed data. Xuyong Lin and Enhua Wang were responsible for conception and supervision of the study and wrote the manuscript. All authors corrected draft versions and approved the final version of the manuscript.

Acknowledgements

We sincerely thank Professor Joachim Kremerskothen for generously providing us with pEGFP-C2, pEGFP-C2-WWC3 plasmids, and pEGFP-C2-WWC3-deltaWW plasmids, and we thank Dr. Hiroshi Kijima for providing the LK2 cell line.

References

1. Meng Z, Moroishi T, Guan KL. Mechanisms of Hippo pathway regulation. Genes Dev. 2016;30(1):1–17.
2. Misra JR, Irvine KD. The Hippo signaling network and its biological functions. Annu Rev Genet. 2018;52:65–87.
3. Harvey KF, Zhang X, Thomas DM. The Hippo pathway and human cancer. Nat Rev Cancer. 2013;13(4):246–57.
4. Ma S, Meng Z, Chen R, Guan KL. The hippo pathway: Biology and pathophysiology. Annu Rev Biochem. 2019;88:577–604.
5. Yu FX, Zhao B, Guan KL. Hippo pathway in organ size control, tissue homeostasis, and cancer. Cell. 2015;163(4):811–28.
6. Nitsch R, Di Palma T, Mascia A, Zannini M. WBP-2, a WW domain binding protein, interacts with the thyroid-specific transcription factor Pax8. Biochem J. 2004;377(Pt 3):553–60.
7. Chen HI, Einbond A, Kwak SJ, Linn H, Koepf E, Peterson S, et al. Characterization of the WW domain of human yes-associated protein and its polyproline-containing ligands. J Biol Chem. 1997;272(27):17070–7.
8. Sudol M. Newcomers to the WW domain-mediated network of the hippo tumor suppressor pathway. Genes Cancer. 2010;1(11):1115–8.
9. McDonald CB, McIntosh SK, Mikles DC, Bhat V, Deegan BJ, Seldeen KL, et al. Biophysical analysis of binding of WW domains of the YAP2 transcriptional regulator to PPxY motifs within WBP1 and WBP2 adaptors. Biochemistry. 2011;50(44):9616–27.

10. Chen S, Wang H, Huang YF, Li ML, Cheng JH, Hu P, et al. WW domain-binding protein 2: an adaptor protein closely linked to the development of breast cancer. Mol Cancer. 2017;16(1):128.
11. Kang SA, Guan JS, Tan HJ, Chu T, Thike AA, Bernadó C, et al. Elevated WBP2 Expression in HER2-positive breast cancers correlates with sensitivity to trastuzumab-based neoadjuvant therapy: A retrospective and multicentric study. Clin Cancer Res. 2019;25(8):2588–600.
12. Dhananjayan SC, Ramamoorthy S, Khan OY, Ismail A, Sun J, Slingerland J, et al. WW domain binding protein-2, an E6-associated protein interacting protein, acts as a coactivator of estrogen and progesterone receptors. Mol Endocrinol. 2006;20(10):2343–54.
13. Buffa L, Saeed AM, Nawaz Z. Molecular mechanism of WW-domain binding protein-2 coactivation function in estrogen receptor signaling. IUBMB Life. 2013;65(1):76–84.
14. Lim SK, Orhant-Prioux M, Toy W, Tan KY, Lim YP. Tyrosine phosphorylation of transcriptional coactivator WW-domain binding protein 2 regulates estrogen receptor α function in breast cancer via the Wnt pathway. FASEB J. 2011;25(9):3004–18.
15. Chen S, Wang H, Li Z, You J, Wu QW, Zhao C, et al. Interaction of WBP2 with ER-alpha increases doxorubicin resistance of breast cancer cells by modulating MDR1 transcription. Br J Cancer. 2018;119(2):182–92.
16. Chan SW, Lim CJ, Huang C, Chong YF, Gunaratne HJ, Hogue KA, et al. WW domain-mediated interaction with Wbp2 is important for the oncogenic property of TAZ. Oncogene. 2011;30(5):600–10.
17. Tabatabaeian H, Rao A, Ramos A, Chu T, Sudol M, Lim YP. The emerging roles of WBP2 oncogene in human cancers. Oncogene. 2020;39(24):4621–35.
18. Lim SK, Lu SY, Kang SA, Tan HJ, Li Z, Adrian Wee ZN, et al. Wnt signaling promotes breast cancer by blocking Itch-mediated degradation of YAP/TAZ transcriptional coactivator WBP2. Cancer Res. 2016;76(21):6278–89.
19. Walko G, Woodhouse S, Pisco AO, Rognoni E, Liakath-Ali K, Lichtenberger BM, et al. A genome-wide screen identifies YAP/WBP2 interplay conferring growth advantage on human epidermal stem cells. Nat Commun. 2017;8:14744.
20. Zhang X, Milton CC, Poon CL, Hong W, Harvey KF. Wbp2 cooperates with Yorkie to drive tissue growth downstream of the Salvador-Warts-Hippo pathway. Cell Death Differ. 2011;18(8):1346–55.
21. Kremerskothen J, Plaas C, Büther K, Finger I, Veltel S, Matanis T, et al. Characterization of KIBRA, a novel WW domain-containing protein. BiochemBiophys Res Commun. 2003;300:862–7.
22. Wennmann DO, Schmitz J, Wehr MC, Krahn MP, Koschmal N, Gromnitza S, et al. Evolutionary and molecular facts link the WWC protein family to Hippo signaling. Mol Biol Evol. 2014;31(7):1710–23.
23. Han Q, Kremerskothen J, Lin X, Zhang X, Rong X, Zhang D, et al. WWC3 inhibits epithelial-mesenchymal transition of lung cancer by activating Hippo-YAP signaling. Onco Targets Ther. 2018;11:2581–91.
24. Han Q, Lin X, Zhang X, Jiang G, Zhang Y, Miao Y, et al. WWC3 regulates the Wnt and Hippo pathways via Dishevelled proteins and large tumour suppressor 1, to suppress lung cancer invasion and

metastasis. J Pathol. 2017;242(4):435–47.

25. Travis WD, Brambilla E, Nicholson AG, Yatabe Y, Austin JHM, Beasley MB, et al. The 2015 World Health Organization classification of lung tumors: Impact of genetic, clinical and radiologic advances since the 2004 classification. J Thorac Oncol. 2015;10(9):1243–60.
26. Lin XY, Zhang XP, Wu JH, Qiu XS, Wang EH. Expression of LATS1 contributes to good prognosis and can negatively regulate YAP oncoprotein in non-small-cell lung cancer. Tumour Biol. 2014;35(7):6435–43.
27. Ren YQ, Wang HJ, Zhang YQ, Liu. YB.WBP2 modulates G1/S transition in ER + breast cancer cells and is a direct target of miR-206. Cancer Chemother Pharmacol. 2017;79(5):1003–11.
28. Li Z, Lim SK, Liang X, Lim YP. The transcriptional coactivator WBP2 primes triple-negative breast cancer cells for responses to Wnt signaling via the JNK/Jun kinase pathway. J Biol Chem. 2018;293(52):20014–28.
29. Song H, Wu T, Xie D, Li D, Hua K, Hu J, et al. WBP2 Downregulation inhibits proliferation by blocking YAP transcription and the EGFR/PI3K/Akt signaling pathway in triple negative breast cancer. Cell Physiol Biochem. 2018;48(5):1968–82.
30. Chen S, Zhang Y, Wang H, Zeng YY, Li Z, Li ML, et al. WW domain-binding protein 2 acts as an oncogene by modulating the activity of the glycolytic enzyme ENO1 in glioma. Cell Death Dis. 2018;9(3):347.
31. Gao J, Dai C, Yu X, Yin XB, Zhou F. microRNA-485-5p inhibits the progression of hepatocellular carcinoma through blocking the WBP2/Wnt signaling pathway. Cell Signal. 2020;66:109466.
32. Ramos A, Miow QH, Liang X, Lin QS, Putti TC, Lim YP. Phosphorylation of E-box binding USF-1 by PI3K/AKT enhances its transcriptional activation of the WBP2 oncogene in breast cancer cells. FASEB J. 2018:fj201801167RR.
33. Field NS, Elbulok OA, Dybas JM, Moser EK, Dar AA, Spruce LA, et al. Itch attenuates CD4 T-cell proliferation in mice by limiting WBP2 protein stability. Eur J Immunol. 2020;50(10):1468–83.
34. Lim SK, Tabatabaeian H, Lu SY, Kang SA, Sundaram GM, Sampath P, et al. Hippo/MST blocks breast cancer by downregulating WBP2 oncogene expression via miRNA processor Dicer. Cell Death Dis. 2020;11(8):669.
35. Lo Sardo F, Strano S, Blandino G. YAP and TAZ in Lung Cancer: Oncogenic Role and Clinical Targeting. Cancers (Basel). 2018;10(5):137.
36. Han Q, Rong X, Wang E, Liu S. WW. and C2 domain-containing protein-3 promoted EBSS-induced apoptosis through inhibiting autophagy in non-small cell lung cancer cells. J Thorac Dis. 2020;12(8):4205–15.
37. Wang Y, Jiang M, Yao Y, Cai Z. WWC3 inhibits glioma cell proliferation through suppressing the Wnt/beta-catenin signaling pathway. DNA Cell Biol. 2018;37(1):31–7.
38. Hou J, Zhou J. WWC3 downregulation correlates with poor prognosis and inhibition of Hippo signaling in human gastric cancer. Onco Targets Ther. 2017;10:2931–42.

Figures

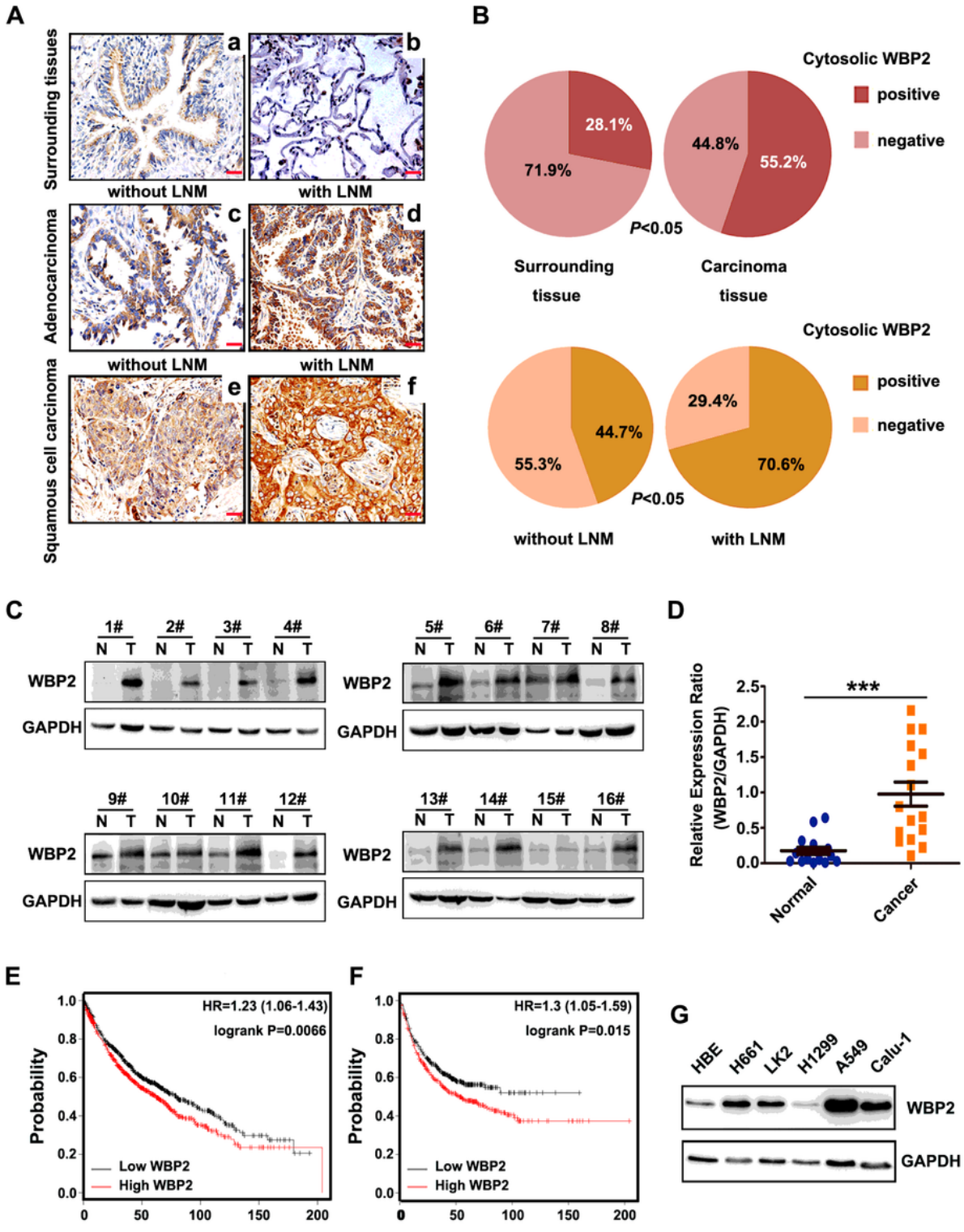

Figure 1

High expression levels of WBP2 in non-small cell lung cancer correlate with poor prognosis A. B: The expression of WBP2 was low or negative in normal bronchial epithelium (A-a) and alveolar epithelium (A-b), positive (+ - + +) in adenocarcinoma (A-c) and squamous cell carcinoma (A-e) without lymph node

metastasis, and strong positive (+ + - + + +) in adenocarcinoma (A-d) and squamous cell carcinoma (A-f) with lymph node metastasis. Magnification: 400×, scale bar: 50 μm. C. D: Western blot analysis revealed that the expression level of WBP2 in lung cancer tissue was significantly higher than that in adjacent normal lung tissue. GAPDH is used as the loading control. E. F: Kaplan¬–Meier plotter network database analysis indicated that the overall survival (OS, E) and progression free survival (FP, F) of lung cancer patients with high expression of WBP2 were significantly lower than those of patients with low expression of WBP2. G: Western blot analysis of expression of WBP2 in the human immortalized bronchial epithelial cell line HBE and in a panel of non-small cell lung cancer cell lines (n = 5). GAPDH was used as a loading control. $P < 0.05$ indicated statistical significance, and ** represented $P < 0.001$.

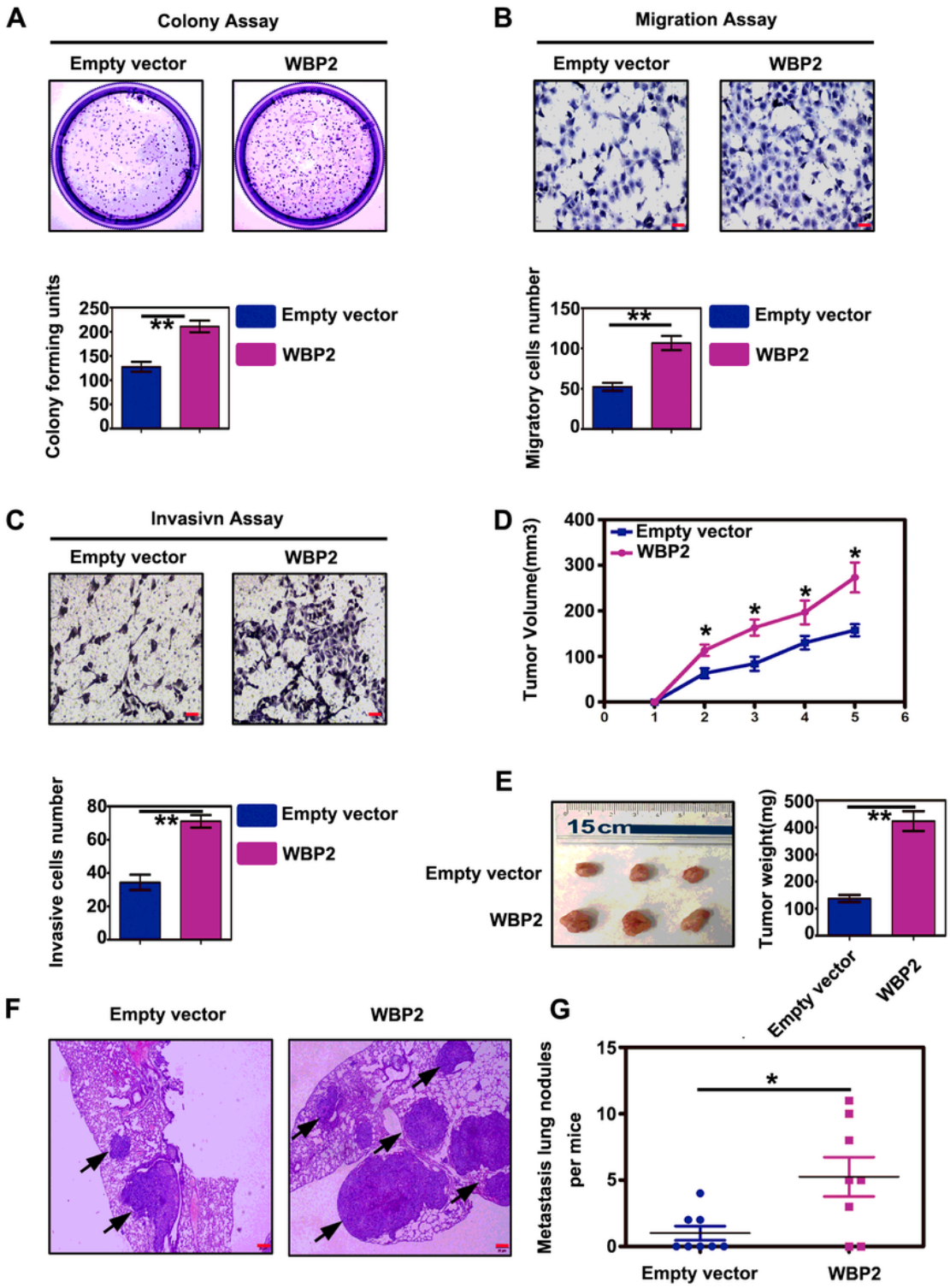

Figure 2

Overexpression of WBP2 promotes the proliferation, invasion, and metastasis of lung cancer cells. A-C: In vivo experiments: the plasmid WBP2 was transfected into the H1299 cell line, and the stable expression monoclonal cells were screened using G418 (800 μg/mL). Colony forming assays and Transwell assays revealed that overexpression of WBP2 protein significantly enhanced the proliferation (A, Control vs WBP2: 127 ± 10 vs 211 ± 12, $P < 0.01$), migration (B, Control vs. WBP2: 52 ± 5 vs 106 ± 8, $P < 0.01$), and

invasiveness (C, Control vs WBP2: 34 ± 4 vs 71 ± 3, P < 0.01) of lung cancer cells D-G: Subcutaneous transplantation tumor experiments and lung metastasis experiments via tail vein injections in nude mice demonstrated that the volumes and weights of subcutaneous transplanted tumors in nude mice were both significantly increased after WBP2 overexpression (D, E, Volume: Control vs. WBP2: 157.7 ± 13.0 vs 273.3 ± 32.8 [mm3], P < 0.05; Weight: Control vs. WBP2: 137.3 ± 13.1 vs. 423.3 ± 36.5 [g], P < 0.01), and the number of lung cancer metastasis foci was also markedly increased (F, G, Control vs WBP2: 1.0 ± 0.5 vs 5.2 ± 1.5, P < 0.05). P < 0.05 indicates statistical significance, * P < 0.05, ** P < 0.01.

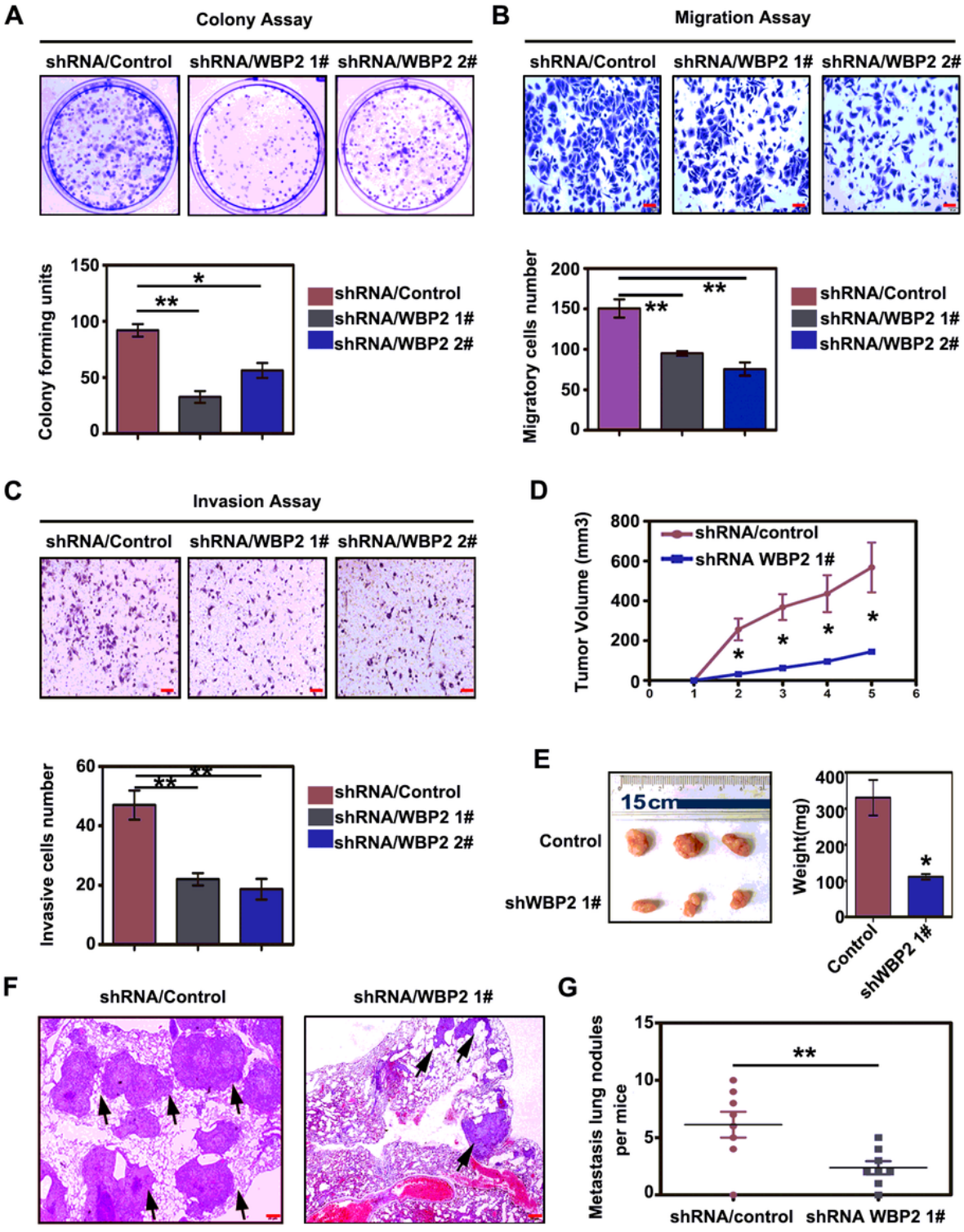

Figure 3

Knockdown of WBP2 weakens the proliferation, invasion, and metastasis abilities of lung cancer cells. In vitro: Lentivirus-coated shRNA-WBP2 was added to the A549 cell line, and the stable cells with knockdown of WBP2 were screened for use of puromycin (5 μg/mL). The colony forming experiment and Transwell assay results demonstrated that the reduction of WBP2 protein significantly weakened the proliferation (A, Control vs. shWBP2-1 vs shWBP2-2: 92 ± 5 vs 32 ± 5 vs 56 ± 6, $P < 0.05$), migration (B, Control vs shWBP2-1 vs shWBP2-2: 150 ± 11 vs 75 ± 8 vs 95 ± 2, $P < 0.01$), and invasiveness (C, Control vs. shWBP2-1 vs shWBP2-2: 47 ± 5 vs 22 ± 2 vs 18 ± 3, $P < 0.01$) of lung cancer cells. In vivo: Subcutaneous transplantation tumor experiments and lung metastasis experiments via tail vein injection in nude mice demonstrated that the volumes and weights of subcutaneous transplanted tumors in nude mice were significantly decreased (D, E□Control vs shWBP2-1: Volume: 568.0 ± 125.3 vs 145.0 ± 9.3 [mm3], $P < 0.05$; Weight:Control vs. shWBP2-1: 330.3 ± 49.2 vs. 111.3 ± 7.5, $P < 0.05$), and the number of lung cancer metastasis foci was also significantly reduced (F, G, Control vs shWBP2-1: 6.1 ± 1.1 vs 2.4 ± 0.6, $P < 0.01$). $P < 0.05$ indicates statistical significance, * $P < 0.05$, ** $P < 0.01$.

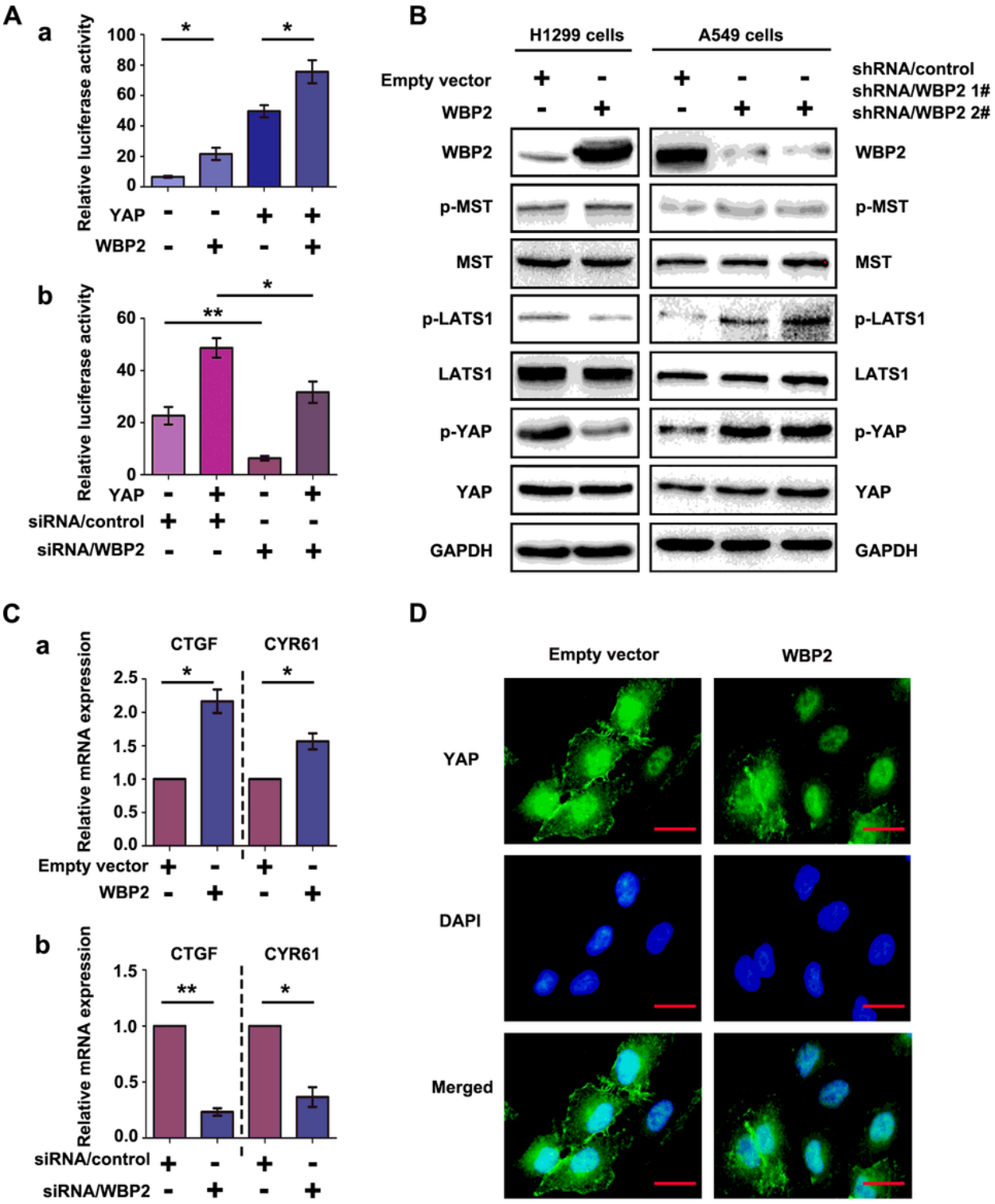

Figure 4

WBP2 is a negative regulator of the Hippo pathway in lung cancer cells A (a-b). WBP2 upregulates the transcriptional activity of the TEAD promoter. The WBP2 plasmid and siRNA-WBP2 were transfected into H1299 and A549 cell lines, respectively. After 48 h, the cells were collected and lysed. Dual-luciferase reporter gene detection revealed that the ectopic expression of WBP2 could significantly upregulate the transcriptional activity of TEAD (A-a), whereas this decreased after WBP2 knockdown (A-b). Transfection

with YAP was used as a stimulus. TK was used as the internal reference. B. WBP2 down-regulated LATS1 phosphorylation and YAP phosphorylation through an MST-independent pathway. After overexpression and knockdown of WBP2 in H1299 and A549 cells, respectively, the phosphorylation and total amount of key proteins in the Hippo pathway were analyzed by western blotting. GAPDH was used as the loading control. C (a-b). The results of RT-qPCR analysis demonstrated that the mRNA levels of CTGF and CYR61 were upregulated after WBP2 overexpression (C-a), and the mRNA levels of these two target genes were downregulated (C-b) after silencing of WBP2. $P < 0.05$ indicates statistical significance, * $P < 0.05$, ** $P < 0.01$. D. Immunofluorescence assay results revealed that the level of YAP nuclear translocation increased in response to overexpression of WBP2 in H1299 cells.

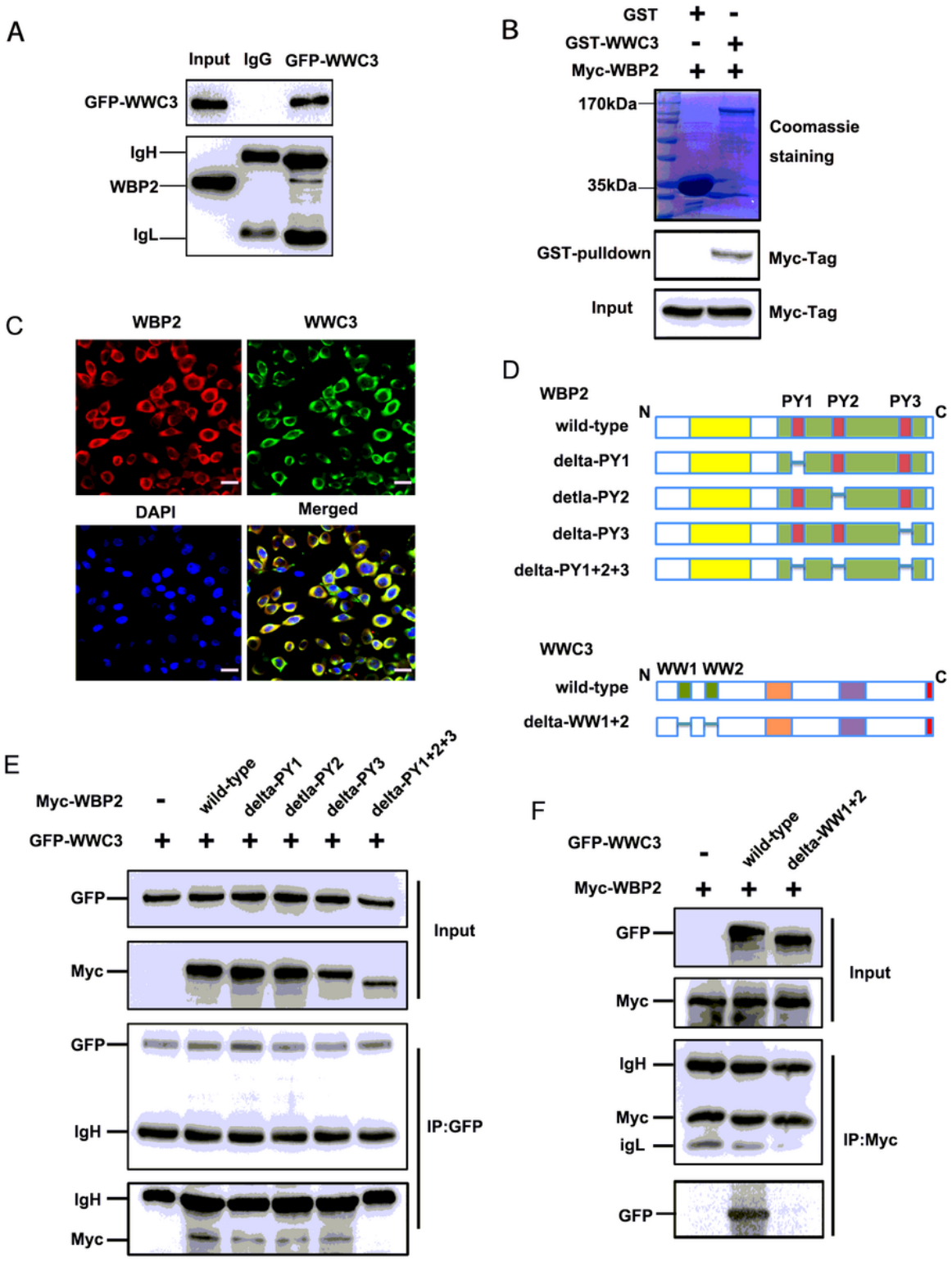

Figure 5

WBP2 interacts with the WW domain of WWC3 via PPxY motifs. A. GFP-WWC3 was transfected into H1299, and after 48 h, the cells were collected and lysed. The GFP monoclonal antibody was used for pull down. The presence of WBP2 in the precipitate was detected by western blot analysis using aWBP2 antibody. B. After incubation with purified GST or GST coupled-WWC3 protein for 6 h at 4 °C, the binding status of the two proteins was examined using Coomassie brilliant blue staining and western blot

analysis. C. Immunofluorescence assay results indicated that WBP2 and WWC3 were co-localized within the cytoplasm of A549 cells. Magnification: 400×, scale bar: 50 μm. D. Schematic diagram of WBP2 and WWC3 splicing mutants. E. GFP-WWC3 and Myc-WBP2 wild-type or a series of mutants were co-transfected into H1299 cells. After 48 h, the cells were collected and lysed. GFP antibody was used for precipitation, and the presence of WBP2 was detected by immunoblotting using Myc antibody. F. Similarly, Myc-WBP2 and GFP-WWC3 wild-type or GFP-WWC3-△WW mutants were co-transfected into H1299 cells. GFP antibody was used for precipitation, and the presence of WBP2 was detected by immunoblotting using Myc antibody.

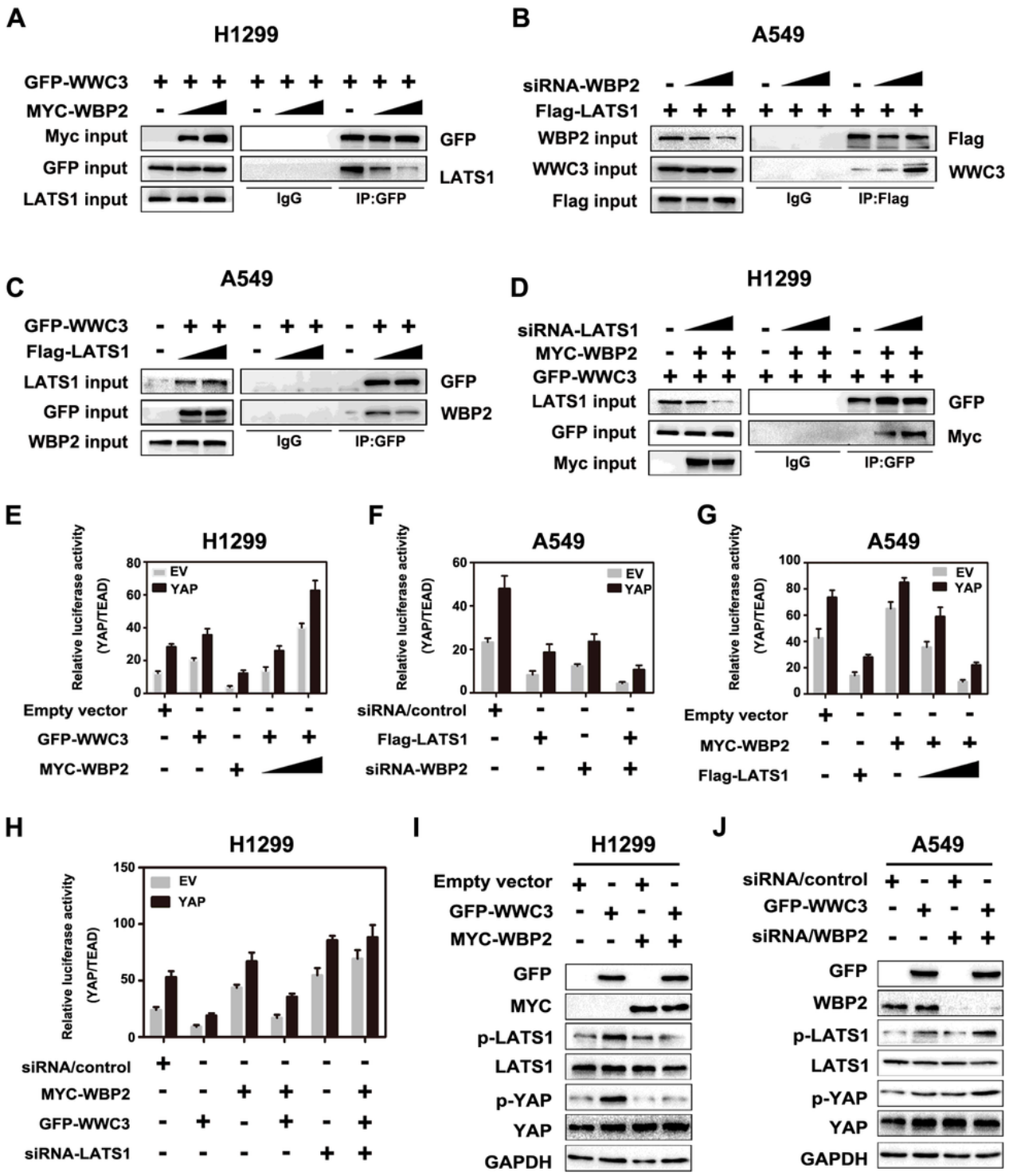

Figure 6

WBP2 and LATS1 competitively bind to WWC3 to inhibit Hippo pathway activity. A. Overexpression of WBP2 attenuated the binding between WWC3 and LATS1. In the H1299 cell line, the WBP2 plasmid (1 μg and 2.5 μg) was transfected in a dose gradient manner. After 48 h, the cells were collected and lysed. GFP monoclonal antibody was used for immunoprecipitation. The combination change of WWC3 and LATS1 protein in the sediment was detected according to western blot. B. The binding of WWC3 to LATS1

increased after WBP2 knockdown. siRNA-WBP2 (5 pmol and 10 pmol) was transfected into A549 cells with high expression of WBP2. After cell collection, the binding was detected according to anti-FLAG immunoprecipitation followed by anti-WWC3immunoblotting. C, D: Conversely, after LATS1 was transfected into A549 cells with low LATS1 expression, the binding of WBP2 to WWC3 gradually decreased with an increase of LATS1 (C). In contrast, the binding of WBP2 to WWC3 gradually increased with the downregulation of LATS1 after siRNA-LATS1 was transfected into H1299 cells with high LATS1 expression (D). E, F: After 48 h post transfection with WBP2 plasmid or siRNA-WBP2 into H1299 cells and A549 cells, the cells were collected and lysed. The results of the dual-luciferase reporter assay revealed that WBP2 overexpression reversed the decrease in TEAD transcriptional activity caused by WWC3 (E). Conversely, WBP2 knockdown further enhanced the decrease in TEAD transcriptional activity caused by WWC3 (F). G, H: Similarly, Dual-luciferase reporter gene detection assays revealed that LATS1 overexpression reversed the WBP2-induced increase in TEAD transcriptional activity (G). Moreover, silencing of LATS1 further enhanced the WBP2-induced increase in TEAD transcriptional activity (H). I, J: Western blot analysis indicated that overexpression of WBP2 reversed the increase in LATS1 and YAP phosphorylation levels induced by WWC3 (I). Conversely, knockdown of WBP2 further increased the phosphorylation levels of LATS1 and YAP (J).

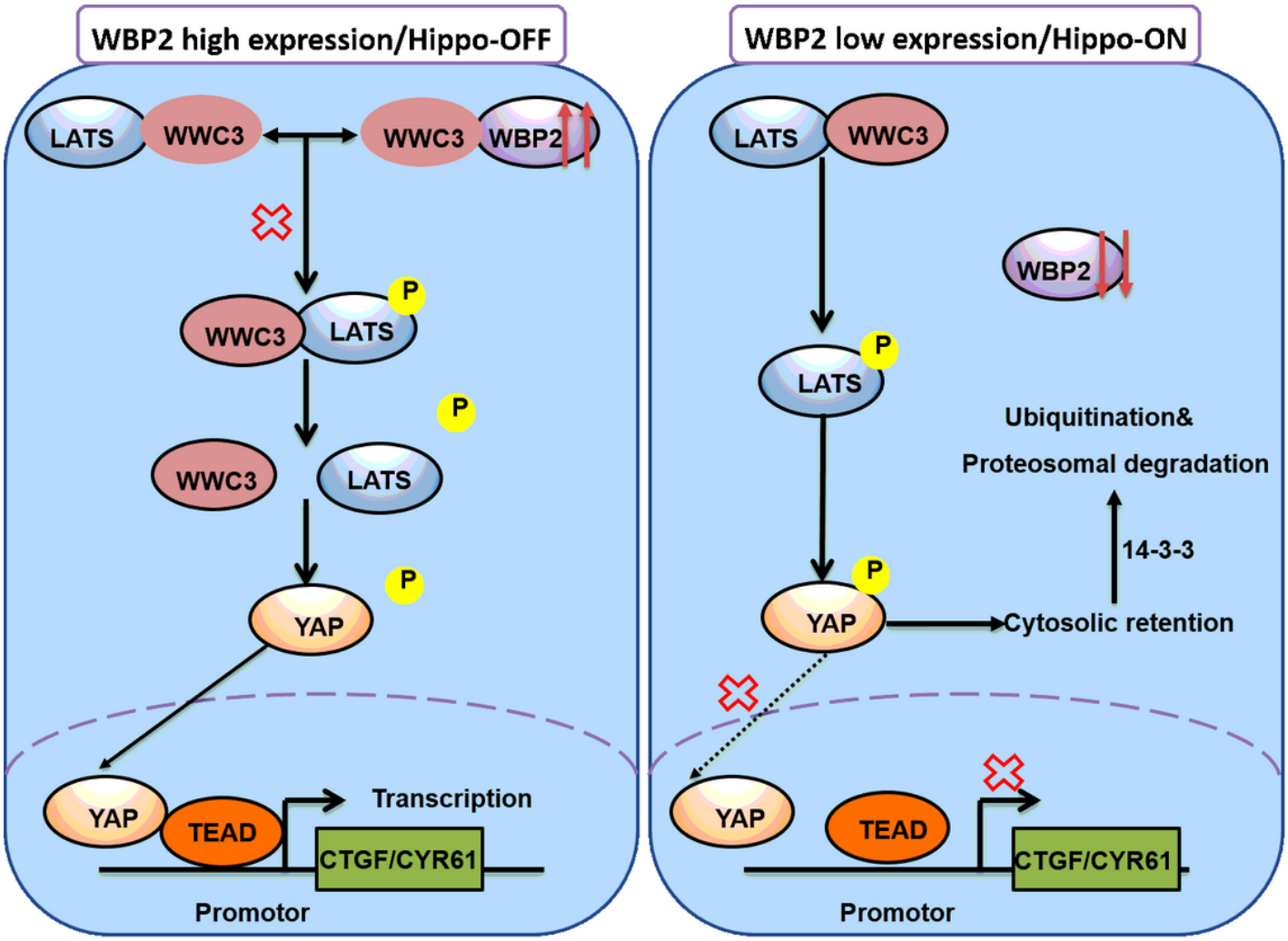

Figure 7

WBP2 is competitive with LATS1 for binding to WWC3, and this competitive binding results in a decrease in WWC3-LATS binding and eventually leads to downregulation of LATS1 phosphorylation to inhibit the activity of the Hippo pathway

Supplementary Files

This is a list of supplementary files associated with this preprint. Click to download.

- SupplementaryFigureS1.tif
- SupplementaryFigureS2.tif
- SupplementaryFigureS3.tif
- SupplementaryFigurelegends.docx